An Experimental Rabbit Torso-tank Setup for Cardiac Rhythms Investigation Using ECGi

A Quadros[1], T Neves[1], V Silva[1], I Sandoval[2], J Paredes[1], I Uzelac[3], J Pachon[4], J Salinet[1]

[1] Center for Engineering, modelling and applied social sciences (CECS), Federal University of ABC (UFABC), São Bernardo do Campo, Brazil
[2] Samsung RD Institute Brazil (SRBR)
[3] Virginia Commonwealth University, Richmond, USA
[4]São Paulo Hospital, São Paulo, Brazil

Abstract

Cardiac diseases are a significant global health concern, with increasing prevalence worldwide. Understanding cardiac electrophysiology is essential for developing effective diagnostic and therapeutic strategies. Optical and electrical mapping techniques provide valuable real-time visualization of electrical activity, particularly in arrhythmias. Electrocardiographic imaging (ECGi) is a promising non-invasive method that estimates cardiac electrical activity without invasive procedures. This study analyzes rabbit heart data using ECGi, demonstrating its reliability and effectiveness in rhythm analysis. The findings support ECGi's potential as a valuable tool for physicians, enhancing strategies for managing cardiac diseases.

1. Introduction

Cardiac diseases are a significant global health concern and the leading cause of death worldwide [1]. Understanding cardiac electrophysiology is crucial for developing effective diagnostic and therapeutic strategies, with optical and electrical mapping playing key roles in deciphering cardiac rhythms [1].

Optical mapping uses fluorescent dyes to visualize and record the electrical activity of cardiac tissue, regarded as the gold standard in cardiac mapping [1]. It provides high spatiotemporal resolution for real-time observation of action potentials and conduction patterns, effectively mapping electrical wave propagation and aiding in the study of arrhythmias and abnormal electrical patterns [2].

Electrical mapping employs electrodes on the heart to directly record electrical signals and includes invasive catheter mapping for detailed local activity and non-invasive body surface mapping (BSPM) to capture signals from the body's surface [3]. Together, these approaches enhance the understanding of cardiac electrophysiology, offering specific insights and broader overviews of cardiac activity.

Electrocardiographic imaging (ECGi) emerges as a promising non-invasive method to estimate the heart's electrical activity without invasive procedures, which is essential given the global burden of cardiac ailments. ECGi requires data collection from torso surface potentials and 3D geometries of the heart and torso surfaces [4]. It surpasses traditional invasive methods, allowing versatile study of cardiac electrical activity and the planning of therapeutic strategies before surgical interventions [5, 6].

This study analyzes rabbit heart data from the developed experimental setup to demonstrate ECGi's reliability and effectiveness in rhythm analysis, contributing to advancements in cardiac electrophysiology and improving management strategies for cardiac diseases.

2. Methodology

Eighteen New Zealand rabbits (3.44 ± 0.36 kg) were used in this study, approved by the local Committee on Ethics in the Use of Animals (CEUA no.3947230519) as detailed in [7]. The animals were anesthetized, euthanized via thoracotomy, and their isolated hearts were connected to the Langendorff system.

The experimental setup for cardiac electrophysiological analysis includes five subsystems: Langendorff system, panoramic optical mapping, epicardial electrical mapping, non-invasive electrical mapping, and 3D geometry construction. Preprocessing techniques were applied after data collection prior to ECGi.

2.1. Experimental setup

Langendorff system: The constant pressure Langendorff perfusion system is essential for simulating physiological conditions in cardiac function studies. It maintains a tem-

perature of 38°C, flow rate of 15-20 mL/min, and pressure of 70 mmHg. Using retrograde Langendorff perfusion through the aorta, it utilizes a modified Krebs-Henseleit solution and continuous carbogen gas bubbling to achieve a pH of 7.82±0.09 and conductivity of 13±1 mS/cm.

Panoramic optical mapping: To obtain optical signals, the setup integrates six deep-red LEDs, focused with condenser lenses and band-pass filtered before reaching the heart's epicardium. The voltage-sensitive dye Di-4-ANBDQPQ is excited by the LEDs, and fluorescence is recorded by three high-speed cameras positioned at 120° angles and equipped with long-pass filters, as shown in Figure 1.

A custom Labview GUI triggers the cameras, acquires images, and saves data for analysis. The resulting data undergoes filtering processes, including baseline correction and spatiotemporal Gaussian smoothing. Processed using Norpix-StreamPix 9 software, the acquired videos provide high-speed, high-resolution insights into heart activity.

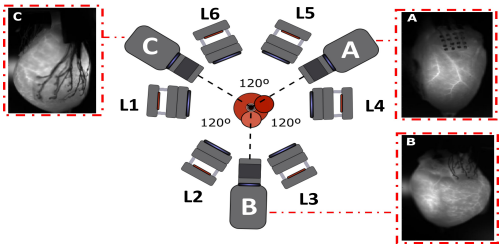

Figure 1. Diagram showing optical mapping setup with three cameras and six LEDs positioned around the rabbit heart, along with captured images from each camera.

Epicardial electrical mapping: To acquire the electrogram (EGM), the electrical mapping system includes three custom-made Microelectrode Arrays (MEAs), each with 16 electrodes. Two MEAs, configured in a 4x4 arrangement of platinum-iridium electrodes from a commercial catheter, are used for atrial mapping and are fixed in a 15x12 mm polyethene terephthalate (PET) square. These atrial MEAs are positioned on the right atrium (RA) and left atrium (LA) epicardium. The third MEA, configured in a 19x22 mm arrangement, is placed on the ventricle (Figure 2A).

Non-invasive electrical mapping:A translucent hexagonal acrylic tank, measuring 18 cm in height with a 5.7 cm face length and 5 mm acrylic thickness, was designed for non-invasive mapping. It features 60 customized stainless-steel electrodes evenly distributed across its faces (10 per face), as shown in Figure 2B. The tank is filled with a sucrose solution circulating at 100 ml/min, maintaining a temperature of 38ºC±1ºC and a pH of 6.8±0.5.

The sucrose solution in the tank mimics the electrical impedance of the animal's body, facilitating the conduction of electrical impulses from the submerged heart. Each electrode (from the MEAs and tank) connects to the Open Ephys electrophysiology amplifier system via an external wire, which includes a 36-pin wire adapter, a 64-channel headstage from Intan, an SPI cable, and an Open Ephys Acquisition board with 12-bit resolution and a 4 kHz sampling frequency.

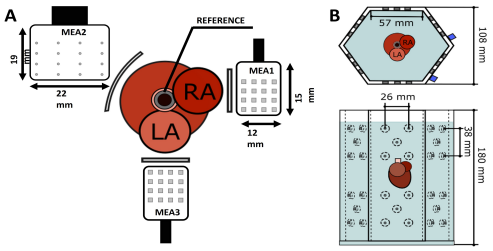

Figure 2. A: Epicardial electrical mapping diagram depicting MEAs and their cardiac positions. B: Tank-torso diagram illustrating dimensions and electrode placements.

3D reconstruction: The 3D geometry reconstruction system for the heart includes a stepper motor, a custom adapter, an Arduino Uno, and an optical camera, all controlled via a LabVIEW Graphical User Interface (GUI) for precise monitoring. The stepper motor rotates the heart 360º, while the optical camera captures images at 3.6° intervals, resulting in 100 total images. After acquisition, Java (ImageJ) processes these images, identifying Regions of Interest (ROI) to create a triangular mesh using the Poisson method based on the identified ROIs.

Electrical signals filtering: Both epicardial (EGM) and non-invasive (tank) signals were filtered using a band-pass filter with cutoff frequencies of 0.5 Hz (high pass) and 250 Hz (low pass). A Notch filter was also applied to attenuate electrical network noise at 60 Hz.

2.2. ECGi

To perform ECGi, two datasets are required: body surface potentials (tank signals) and geometries (heart and torso-tank). The heart geometry is generated during the experiment, while the 3D tank geometry is constructed by manually measuring the positions of 12 vertices and 60 non-invasive electrodes. The 60 tank signals were processed using Laplacian interpolation, which estimates values from known data points to maintain smoothness [8]. This method increased the number of signals to match the 218 vertices of the generated tank.

Transfer matrix: The next step in the ECGi procedure involves discretizing the heart and torso surfaces into triangular elements, enabling a linear model to represent the relationship between torso and heart potentials, resulting in the transfer matrix [4, 6]. Generated by Boundary El-

ement Methods (BEM), this matrix incorporates the geometric information and electrophysiological properties of the volume conductor connecting the two surfaces [6].

Regularization method: The inverse problem of electrocardiography is unstable due to its ill-posed nature, where small variations in torso signal measurements or geometry can lead to significant errors in calculating cardiac potentials [4,9]. To achieve unique and stable solutions, we employed Truncated Singular Value Decomposition (TSVD) regularization (order 0) in this study. TSVD stabilizes the solution by decomposing the transfer matrix into singular values and vectors, truncating smaller values associated with noise to reduce the influence of unstable components. This allows for the reconstruction of cardiac potentials using only the most significant, stable components [10].

2.3. Metrics

Five metrics were extracted to analyze and evaluate ECGi performance:

Dominant Frequency (DF): Computed using Fast Fourier Transform (FFT) analysis, DF identifies the primary frequency component for comparing optical, EGM, and rEGM signals.

Local Activation Time (LAT): Calculated for both EGM and rEGM using the -dV/dt method.

Euclidean Distance: Measures the straight-line distance between two points [11]. In this study, it compared the locations of the earliest activations in EGM and rEGM.

Root Mean Squared Error (RMSE): Quantifies differences between EGM and rEGM, serving as a metric for estimation accuracy; lower RMSE values indicate better agreement [12].

Cross-Correlation (CC): Assesses the similarity between two signals over time-lag and is commonly used in ECGi validation to evaluate shape accuracy [5]. MATLAB's `xcorr` function computed the correlation and identified the time shift that maximized the correlation coefficient between EGM and rEGM.

3. Results and discussion

Figure 3 shows a 2-second segment of regular ventricular tachycardia, including two optical and EGM ventricular signals alongside two tank signals, all exhibiting a frequency around 5 Hz. Both optical and electrical signals display clear ventricular activations with strong coherence. The tank signals effectively capture these activations, indicating good signal propagation, although their amplitude is smaller than that of the EGM due to signal attenuation as it travels to the tank walls. The first tank signal at the top and the second below the heart illustrate opposing signal directions, reflecting the heart's central position within the tank.

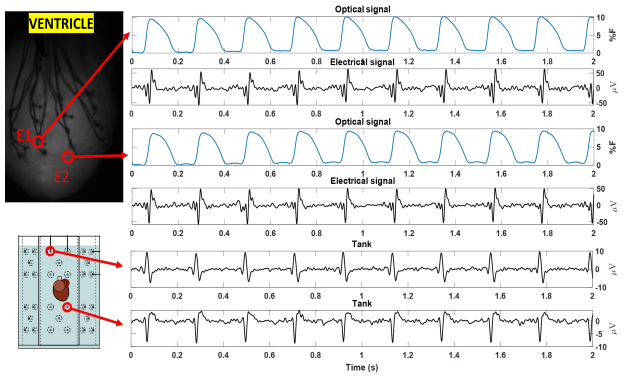

Figure 3. 2 seconds segment of optical, EGM and tank signals during ventricular tachycardia simultaneously collected.

After estimating using ECGi, the recording was mapped onto the 3D geometry (Figure 4), highlighting the ventricular region. A 2D potential map from EGM was plotted for comparison; although the ranges differ, both maps indicate potentials close to zero. A 2-second segment of rEGM from two ventricular points shows distinct activations, with varying amplitudes likely due to optimization parameters of the regularization method, highlighting ECGi's sensitivity to amplitude variations. While the tachycardia rhythm is evident, some noise is observed between activations.

Cross-correlation analysis between EGM (black) and rEGM (red) for highlighted electrodes revealed a correlation of 0.86 for electrode E2, with minor morphological discrepancies. Electrode EL3 had a lower correlation of 0.81 and a lag of 1.5 ms. E4 achieved a correlation of 0.87 with a lag of 4.35 ms, while E5 showed the highest correlation of 0.91 but also the largest delay of 4.5 ms. Notably, rEGM amplitudes were at least twice as large.

The RMSE for the ventricular region was 7 at its lowest and averaged 35.47, indicating that despite high correlations, amplitude and time delay differences impacted the metric. The earliest rEGM activation point was detected 27.75 ms later than the EGM, located 6 mm away.

Dominant frequency maps comparing optical, EGM, and rEGM signals in the ventricular region (Figure 5) all show a DF close to 5 Hz. The average DF was 4.725 ± 9e-14 Hz for optical signals, 4.78 ± 0.2 Hz for EGM, and 4.9 ± 0.01 Hz for rEGM, demonstrating good concordance between the signals.

4. Conclusion

This study employed an experimental setup with rabbit hearts to evaluate ECGi's performance during ventricular tachycardia. ECGi serves as a valuable tool for understanding cardiac rhythms and abnormalities by estimating surface electrical activity. The strong similarity between

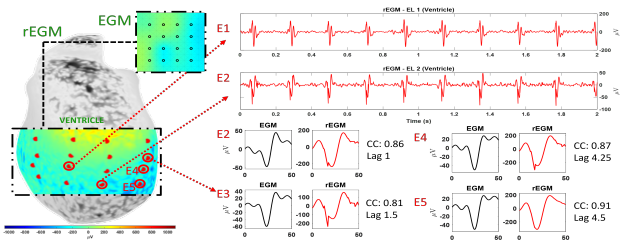

Figure 4. On the left, a 3D potential map from ECGi signals is presented alongside a 2D potential map from simultaneous ventricular EGM. The top right features a 2-second segment of two rEGM signals from the ventricle, while the bottom right compares EGM and rEGM signals over 50 ms, including the cross-correlation and time lag (in ms) for four electrodes.

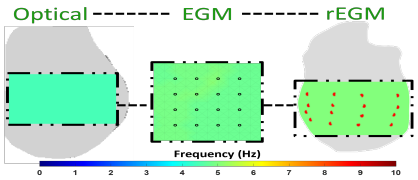

Figure 5. Dominant frequency maps comparing optical, EGM, and rEGM signals in the ventricular region, all indicating a dominant frequency close to 5 Hz.

EGM and rEGM signals, supported by computed metrics, underscores ECGi's potential for providing detailed spatial and temporal insights into cardiac activity. However, discrepancies in CC, RMSE, and LAT analyses highlight the need for refinements to improve accuracy and reliability.

Acknowledgments

A. Quadros, T. Neves and J. Siles, are supported by FAPESP grant 2023/06306-6, 2024/02521-2 and 2020/03601-9, respectively. I. Uzelac and J. Salinet are supported by grant 2018/25606-2 FAPESP. This study is supported by CNPq INCT INTERAS. call 58/2022.

References

[1] Lombello CB, da Ana PA. Current Trends in Biomedical Engineering. Springer Nature, 2023.

[2] Berenfeld O, Ennis S, Hwang E, Hooven B, Grzeda K, Mironov S, Yamazaki M, Kalifa J, Jalife J. Time- and Frequency-Domain Analyses of Atrial Fibrillation Activation Rate: The Optical Mapping Reference. Heart Rhythm 2011;8(11):1758–1765.

[3] Coveney S, Cantwell C, Roney C. Atrial Conduction Velocity Mapping: Clinical Tools, Algorithms And Approaches For Understanding The Arrhythmogenic Substrate. Medical Biological Engineering Computing 2022;60(9):2463–2478.

[4] Rudy Y. Noninvasive Electrocardiographic Imaging Of Arrhythmogenic Substrates In Humans. Circulation research 2013;112(5):863–874.

[5] Cluitmans M, Brooks DH, MacLeod R, Dössel O, Guillem MS, Van Dam PM, Svehlikova J, He B, Sapp J, Wang L, et al. Validation And Opportunities Of Electrocardiographic Imaging: From Technical Achievements To Clinical Applications. Frontiers in physiology 2018;9:1305.

[6] Salinet J, Molero R, Schlindwein FS, Karel J, Rodrigo M, Rojo-Álvarez JL, Berenfeld O, Climent AM, Zenger B, Vanheusden F, et al. Electrocardiographic Imaging For Atrial Fibrillation: A Perspective From Computer Models And Animal Experiments To Clinical Value. Frontiers in physiology 2021;12:653013.

[7] Siles J, Uzelac I, Silva V, Sandoval I, Weber G, Salinet J. Simultaneous Recording of Electrical and Panoramic Optical Mapping From Ex-vivo Isolated Rabbit Hearts: From Sinus Rhythm to Induced Arrhythmia. In 2023 Computing in Cardiology (CinC), volume 50. IEEE, 2023; 1–4.

[8] Oostendorp TF, van Oosterom A, Huiskamp G. Interpolation On A Triangulated 3D Surface. Journal of Computational Physics 1989;80(2):331–343.

[9] Colli-Franzone P, Guerri L, Tentoni S, Viganotti C, Baruffi S, Spaggiari S, Taccardi B. A Mathematical Procedure For Solving The Inverse Potential Problem Of Electrocardiography: Analysis Of The Time-Space Accuracy From In Vitro Experimental Data. Mathematical Biosciences 1985; 77(1-2):353–396.

[10] Figuera C, Suárez-Gutiérrez V, Hernández-Romero I, Rodrigo M, Liberos A, Atienza F, Guillem MS, Barquero-Pérez Ó, Climent AM, Alonso-Atienza F. Regularization Techniques For ECG Imaging During Atrial Fibrillation: A Computational Study. Frontiers in physiology 2016;7:466.

[11] Potse M, Vinet A, Opthof T, van Dam P, Boukens BJ, Coronel R. Validation Of ECGI For Activation Mapping In A Novel Isolated Canine Heart Preparation. PloS one 2017; 12(3):e0172725.

[12] Smith LI. A Tutorial On Principal Components Analysis 2002;.

Address for correspondence:

Angélica Drielly Santos de Quadros
Alameda da Universidade, s/n - Anchieta, São Paulo, Brazil
angelica.drielly@ufabc.edu.br